Electrochimica Acta 107 (2013) 216–224

Contents lists available at ScienceDirect

Electrochimica Acta

journal homepage: www.elsevier.com/locate/electacta

Electrocatalytic oxidation of methanol on Ru deposited NiZn catalyst at graphite in alkaline medium

Esra Telli[a,*], Ali Döner[b], Gülfeza Kardaş[b]

[a] Osmaniye Korkut Ata University, The Faculty of Engineering, Energy Systems Engineering Department, 80000 Osmaniye, Turkey
[b] Çukurova University, Science and Letters Faculty, Chemistry Department, 01330 Adana, Turkey

ARTICLE INFO

Article history:
Received 5 December 2012
Received in revised form 14 May 2013
Accepted 21 May 2013
Available online 3 June 2013

Keywords:
Methanol
Alkaline medium
Electrocatalysis
Graphite
Ruthenium

ABSTRACT

The methanol oxidation on C/NiZn-Ru electrode in a 1.00 M KOH and 1.00 M KOH + 1.00 M methanol solutions at different scan rates and temperatures was studied by the cyclic voltammetry (CV), electrochemical impedance spectroscopy (EIS) and chronoamperometry (CA) techniques. The graphite electrode is coated in a nickel–zinc bath by electrodeposition for use as anode materials for methanol oxidation in alkaline solutions. It is etched in a concentrated alkaline solution to produce a porous and electrocatalytic surface suitable for use in the methanol oxidation (C/NiZn). Ruthenium was electrodeposited on a C/NiZn electrode. The surface morphologies and compositions of electrodes were determined by energy dispersive X-ray (EDX) and scanning electron microscopy (SEM). Kinetic parameters of oxidation such as the anodic electron transfer coefficient (α_a), cathodic electron transfer coefficient (α_c), charge transfer rate constant (k_s) and activation energy values were calculated. The effect of methanol concentration on methanol oxidation were also investigated. It was found that the ruthenium electrodeposited electrode showed higher catalytic activity and stability toward methanol oxidation than the C/NiZn electrode.

1. Introduction

In recent years, direct methanol fuel cells (DMFCs) have gained interest due to the advantages of liquid fuel's low operating temperature, easy transportation and storage, high-energy efficiency, low-exhaust and fast start-up time [1]. Because alkaline fuel cells have higher overpotential (200–300 mV) and lower oxidation current, they are not widely used due to limited electrochemical kinetics. Thus various studies have focused on increasing methanol oxidation reaction efficiency (MOR) in DMFCs [2–6].

Carbon has been used for many years as a support material for industrial valuable metal catalysts, activated carbon, carbon black, graphite and graphitic materials, which have been suitable for different catalytic processes. The electronic conducting properties of carbon provide performance benefits for fuel cells [7]. Because of its porous structure, electrical conductivity and large surface area, carbon prefers to act as a supporting electrocatalyst in direct alcohol fuel cells [8]. The electrode surface area should be large for catalytic oxidation. Therefore, carbon-supported electrodes, such as Pt–Ru–P/carbon nano-composites, Pt–Ru, Pt/Ni and Pt/Ru/Ni alloy nanoparticles are commonly used. The combination of a large surface area with an enhanced catalytic activity and low overpotential enables codeposits of transition metals and oxides on the graphite substrate [9,10]. It is well established that nickel can be used as a catalyst due to its surface oxidation properties. Nickel composite electrodes have previously been used as catalysts in fuel cells [11–15]. Several researchers reported that Ni and its alloy could act as effective catalysts for the oxidation of methanol. Due to the formation of nickel oxyhydroxide (NiOOH) during the oxidation of Ni in alkaline media, it shows significant electrocatalytic activity for alcohol oxidation [4]. Nickel and its alloys are the most studied electrode materials for alkaline media. Various zinc-based alloys prepared by leaching of Zn have also been studied and reported. The caustic leaching of Zn is accompanied by volume loss followed by porous and crack formation, yielding a highly porous catalytic surface suitable as a very effective catalysts for the hydrogen evolution reaction [16–20]. C/NiZn and C/NiZn-Ru electrodes' electrocatalytic activities were investigated. These electrodes's catalytic roles for methanol oxidation reaction were compared with cyclic voltammetry (CV), electrochemical impedance spectroscopy (EIS) and chronoamperometry (CA) techniques.

2. Experimental

The graphite electrodes were cut from a cylindrical rod to a length of 5 cm and coated with polyester to a surface area of 0.283 cm^2. The electrical conductivity was provided by a copper wire. Before deposition, the electrode surface was polished with

* Corresponding author. Tel.: +90 328 8271000 3557.
E-mail address: esrademir1@gmail.com (E. Telli).

0013-4686/$ – see front matter © 2013 Elsevier Ltd. All rights reserved.
http://dx.doi.org/10.1016/j.electacta.2013.05.113

emery paper (320–1200 grain size), then washed with distilled water and immersed into a bath solution [21]. The nickel bath composition was 30.00% $NiSO_4$, 1.00% $NiCl_2$ and 1.25% H_3BO_3 and was formed by addition of 1, 3, 5, 7, 10 and 15% $ZnSO_4{\cdot}7H_2O$ in nickel bath. The electrodeposition of the nickel-zinc coating was performed galvanostatically using a potentiostate–galvanostate instrument (Princeton Applied Research Model 362) with a three electrode configuration. A nickel electrode was used as counter electrode and Ag/AgCl was used as the reference electrode. The electrodes were coated by a bath solution mixed at a constant speed at room temperature. Coating thickness was determined approximately by Faraday's laws. A constant current density of 100 mA cm^{-2} was applied to the electrolysis system for 544 s during the electrodeposition [19]. After deposition, the electrodes were rinsed with distilled water in order to remove residues of bath chemicals and unattached particles. The electrodes were, first treated with 1 M NaOH for several hours until the dissolution rate of Zn decreased. The electrodes were then exposed to 30% NaOH solution at room temperature for 24 h until no hydrogen bubbling was observed. These treatments promote a partial leaching of the Zn producing a porous electrode of high surface area. The electrode was washed with distilled water. CVs were obtained in 1.00 M KOH and 1.00 M KOH + 1.00 M methanol solution at 100 mV s^{-1} scan rate by the created electrodes. The electrode % 10 $ZnSO_4{\cdot}7H_2O$ bath showed a higher peak current than other electrodes, and obtained 1, 3, 5, 7 and 15% $ZnSO_4{\cdot}7H_2O$. The experiments were repeated three times. The bath with 10% $ZnSO_4{\cdot}7H_2O$ was used for the electrodeposition of ruthenium. The alkaline leached C/NiZn electrode was immersed in a properly prepared Ru bath and theoretically 1 mg cm^{-2} Ru was loaded electrochemically over the alkaline leached porous NiZn layer. The chemical composition of Ru bath was 0.032 g $RuCl_3{\cdot}H_2O$ and 0.10 M KCl. In the case of Ru loading, a Pt anode was used and 3.50 mA cm^{-2} current density was applied to the electrolysis system for 1 h ensuring that all of the Ru^{3+} ions were completely reduced to their metallic forms. The electrode was washed with distilled water and used for further electrochemical measurements.

The electrochemical measurements were carried out using a CHI 604 model computer-controlled electrochemical analyzer with serial number 6A721A. A double-wall-one-compartment cell with a three electrode configuration was used. A platinum sheet (with 2 cm^2 surface area), an Ag/AgCl electrode and the prepared electrodes were used as the auxiliary, the reference and the working electrodes, respectively. All potential values were referred to the reference electrode. Electrochemical impedance spectroscopy (EIS) and chronoamperometry (CA) measurements were performed at a constant potential. The frequency range was between 10^5 and 10^{-3} Hz and the amplitude was 5 mV for EIS measurements.

The test solutions used in this study were 1.00 M KOH (Merck) solution with and without addition of various methanol concentrations (Merck). All the tests were carried out at 298 K and the test solutions were opened to the air. The tests were prepared by using bidistilled water. The elemental analysis of C/NiZn and C/NiZn-Ru were determined by EDX analysis. The surface morphologies were investigated by SEM technique using a Carl Zeiss Evo 40 SEM instrument at high vacuum and 10 kV EHT.

3. Results and discussion

3.1. Characterization

Fig. 1 shows the CVs of C, C/Ni, C/NiZn and C/NiZn-Ru in 1.00 M KOH solution at 298 K between the hydrogen and oxygen evolution potential range. Fig. 1 describes the process of carbonization

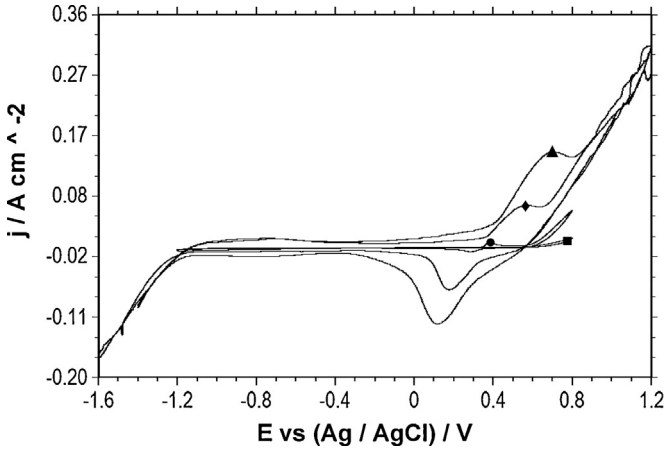

Fig. 1. Cyclic voltammograms of C (■), C/Ni (●), C/NiZn (♦) and C/NiZn-Ru (▲) in 1.00 M KOH at 298 K (scan rate: 100 mV s^{-1}).

on the graphite surface in the alkaline media. When the graphite surface was coated with the nickel, the CV of the graphite changed. Anodic and cathodic peaks at the CV can be seen. These peaks are related to $Ni(OH)_2/NiOOH$ formation. In Fig. 1, the peak at −0.80 V corresponds to Ni/Ni^{2+} oxidation [22,23], the transformation of α-$Ni(OH)_2$ to β-$Ni(OH)_2$ takes place between the potential ranges of −0.60 to 0.30 V [24]. The peak centered at 0.40 V corresponds to the Ni^{2+}/Ni^{3+} transition [24–26]. The cathodic peak at 0.28 V corresponds to the Ni^{3+}/Ni^{2+} reduction. In Fig. 1, anodic and cathodic peak intensity at the CVs of the C/NiZn and C/NiZn-Ru catalyst changes by changing the composition of Ni in the catalyst. Ni^{2+}/Ni^{3+} oxidation peak current values were obtained for C/Ni, C/NiZn and C/NiZn-Ru electrodes as 8.8×10^{-3}, 53×10^{-3} and 150×10^{-3} A cm^{-2}, respectively.

The surface morphology of the electrodes was analyzed by scanning electron microscopy (SEM). The SEM images of graphite (C), nickel coated graphite (C/Ni), nickel zinc coated graphite (C/NiZn*), after alkaline leaching nickel–zinc coated graphite (C/NiZn) and C/NiZn-Ru electrodes are shown in Fig. 2. The films are fairly compact with virtually no pores and cavities as shown in Fig. 2a and b. It can be seen that the surface of the graphite was fully covered by the NiZn electrochemical deposition as shown in Fig. 2c. Moreover, the coating is compact with smooth and low porous structure. However, the morphology of surface changed significantly after leaching of zinc from the deposit. Fig. 2d shows large-sized particles with cracked surfaces. From comparison of Fig. 2c and d, a great number of cracks and pores appeared to lead a high surface area available for the MOR. The surface morphology of the C/NiZn electrode is observed to change with addition of ruthenium. The surface is porous in Fig. 2e. C/NiZn-Ru electrode surface is seen bright.

Fig. 3 presents energy dispersive X-ray (EDX) spectrum obtained from the surface of C/Ni, C/NiZn*, C/NiZn and C/NiZn-Ru electrodes. The composition of C/Ni electrode is given as 85.30 wt% Ni and 14.70 wt% C in Fig. 3a. Fig. 3b shows the EDX analysis of C/NiZn* electrode, which reveals that the plating layer is compose of Ni and Zn elements with percentages of 20.76 wt% C, 7.04 wt% Ni and 72.20 wt% Zn. However, these percentages are altered after the leaching of zinc from the surface of the electrode. EDX analysis of C/NiZn electrode results was presented in Fig. 3c to be 7.19 wt% Ni, 2.58 wt% Zn, 90.23 wt% C. This low Zn content supports the porous structure as supported by the SEM image. The composition of C/NiZn-Ru electrode is given as 32.29 wt% C, 46.62 wt% Ni, 20.95 wt% Zn and 0.14 wt% Ru in Fig. 3d.

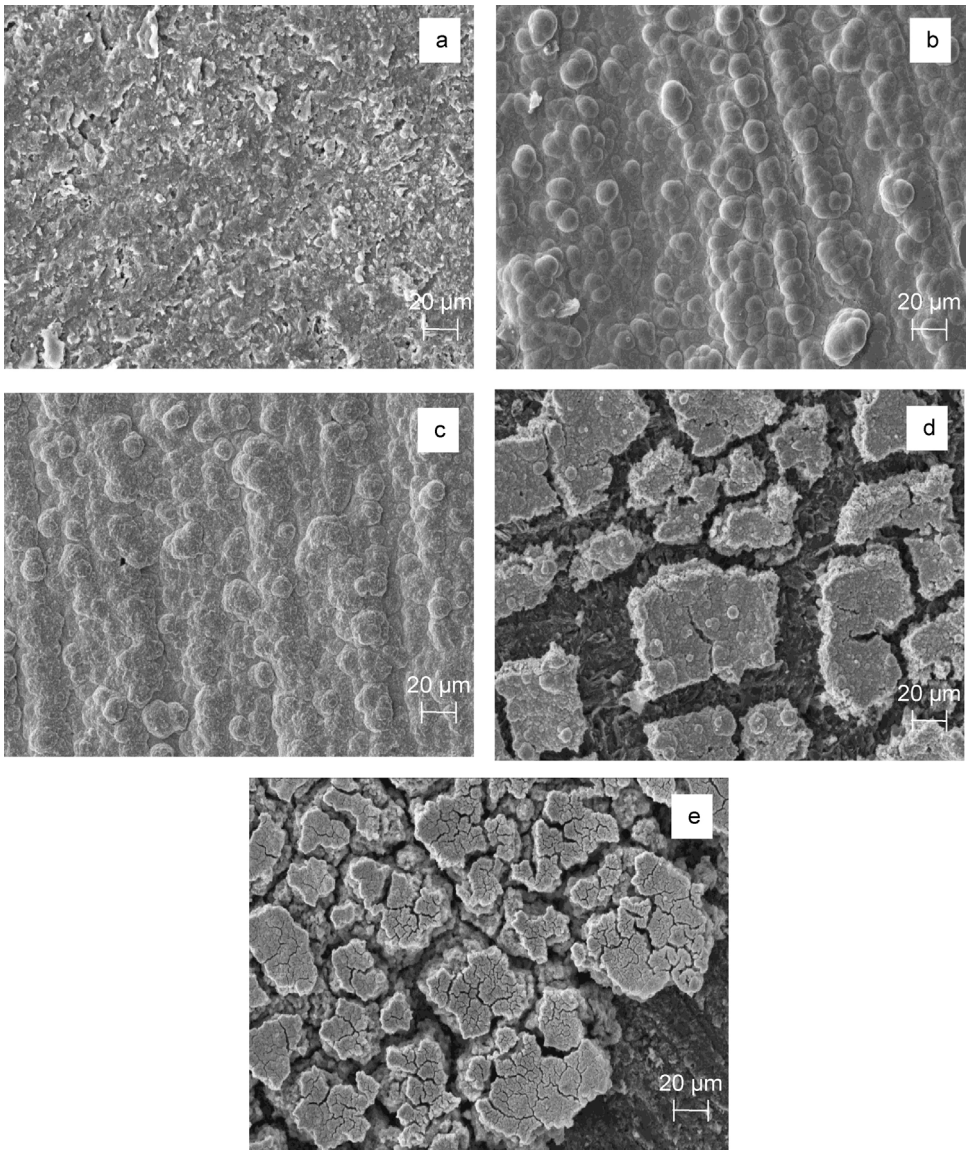

Fig. 2. SEM images of C (a), C/Ni (b), C/NiZn* (c), C/NiZn (d), C/NiZn-Ru (e) electrodes.

3.2. Electrooxidation of methanol on modified electrodes

The cyclic voltammogram (CV) in Fig. 4 shows the methanol oxidation on C, C/Ni, C/NiZn and C/NiZn-Ru electrodes. Inset of Fig. 4 shows CVs of C/NiZn-Ru in 1.00 M KOH (●) and in 1.00 M CH_3OH + 1.00 M KOH (▲) at 298 K (scan rate: 100 mV s^{-1}). Methanol oxidation peak current density value is considerably higher than the observed value of the methanol-free environment. From the curve, (■) in Fig. 4, no current peak of methanol oxidation is observed, indicating that the graphite electrode has no obvious electrocatalytic activity for methanol oxidation. It is clear from Fig. 4(●), (♦) and (▲) that two well-defined anodic peaks and one cathodic peak were observed in the forward and backward scan, for the C/Ni, C/NiZn and C/NiZn-Ru electrodes. As recently reported in literatures [27–32], this behavior is typical oxidation behavior of CH_3OH as follows:

$$Ni(OH)_2 + OH^- \Leftrightarrow NiOOH + H_2O + e^- \quad (1)$$

$$NiOOH + CH_3OH \rightarrow Ni(OH)_2 + \text{products} \quad (2)$$

Ni^{2+}/Ni^{3+} oxidation peak is seen at −0.80 V, approximately. As shown in Fig. 4, a relatively fast increase in the kinetics is followed by even faster deactivation, with the formation of current maximum at the potentials,

$$CH_3OH_{sol} \xrightarrow{k_1} CH_3OH_{ad} \xrightarrow{k_2} CO_{ad} + 4H^+ + 4e^- \quad (3)$$

and the rate of oxidation of dehydrogenation products (CO_{ad} in Eq. (3)) with oxygen-containing species (symbolized by OH_{ad}); in alkaline solutions [33]

$$CO_{ad} + 2OH_{ad} + 3OH^- \xrightarrow{k_3} CO_3^{2-} + 2H_2O + e^- \quad (4)$$

Ruthenium converts to Ru-OH in alkaline medium [34,35].

$$Ru + H_2O \Leftrightarrow Ru\text{–}OH + H^+ + e^- \quad (5)$$

The following reaction takes place in methanol:

$$Ru\text{–}OH + CH_3OH \Leftrightarrow Ru\text{–}OCH_{3ad} + H_2O \quad (6)$$

The RuO_2 oxidation mechanism is given as follows according to literature [36,37]:

$$RuO \cdot xH_2O \rightarrow RuO(OH)(x-y)H_2O + 2H_2O + H^+ + e^- \quad (7)$$

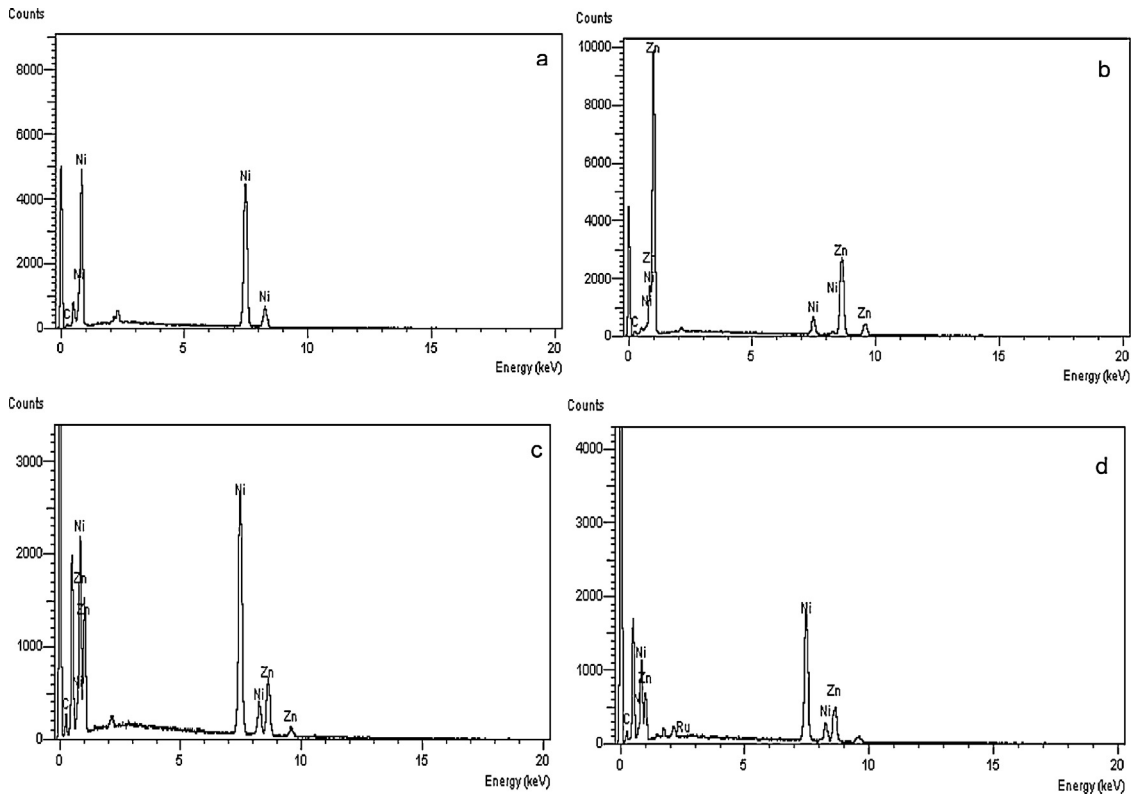

Fig. 3. EDX spectrums of C/Ni (a), C/NiZn* (b), C/NiZn (c), C/NiZn-Ru (d) electrodes.

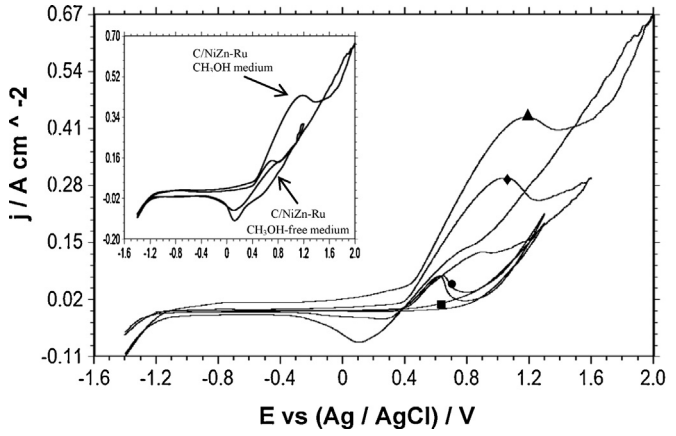

Fig. 4. Cyclic voltammograms for the methanol oxidation reaction on C (■), C/Ni (●), C/NiZn (♦) and C/NiZn-Ru (▲) electrodes at scan rates of 100 mV s^{-1} in 1.00 M CH_3OH + 1.00 M KOH at 298 K. Inset: CVs of C/NiZn-Ru in 1.00 M KOH (●) and in 1.00 M CH_3OH + 1.00 M KOH (▲) at 298 K (scan rate: 100 mV s^{-1}).

$$RuO(OH)(x-y)H_2O \rightarrow RuO_2(x-y)(H_2O) + H^+ + e^- \quad (8)$$

$$RuO_2(x-y)(H_2O) \rightarrow RuO_3 + zOH^- + (z+2)H^+ + 2e^- \quad (9)$$

In this study, from Ru^{2+} to Ru^{6+} transition mechanism which only hydrogen participates in the RuO_2 charging processes attributes as,

$$RuO \cdot xH_2O \rightarrow RuO(OH)(x-y)H_2O + H^+ + e^- \quad (10)$$

$$RuO(OH) \cdot xH_2O \rightarrow RuO_2 \cdot xH_2O + H^+ + e^- \quad (11)$$

$$RuO_2 \cdot xH_2O \rightarrow RuO_3(x-y)H_2O + 2H^+ + 2e^- \quad (12)$$

In addition, ruthenium deposited electrodes shown a high catalytic effect for methanol oxidation reaction were indicated at the previous studies [37–44]. All adsorbed intermediates, and surface reactions are clarified by bifunctional mechanism [45,46]. The bifunctional mechanism recommends that foreign metal (M) supports water dissociation at lower potentials,

$$M + H_2O \leftrightarrow M(OH)_{ad.} + H^+ + e^- \quad (13)$$

or

$$M + H_2O \leftrightarrow M(H_2O)_{ad.} \quad (14)$$

Langmuir–Hinshelwood mechanism supports the oxidation of species produced at reactions (13) and (14) [47]. Furthermore, this mechanism explains transport for oxidation of adsorbed CO and oxygen at the electrode surface in the electrolyte [48]. Oxidation of adsorbed CO molecules takes places in two steps: (1) water decomposes on ruthenium electrode and adsorbed OH, which commenced oxidation of CO molecules is generated at the electrode surface (Eq. (13)) (2) adsorbed OH_{ad} and CO_{ad} molecules react (Eq. (14)) [49]:

$$CO_{ad.} + OH_{ad.} \xrightarrow{rds} CO_2 + H^+ + e^- \quad (15)$$

Additionally, ruthenium deposition at the electrode surface for methanol oxidation is explained by two theories in literature: The bifunctional mechanism [50,51], and the ligand model [52–55]. Ruthenium addition activates water molecules to produce Ru–OH on the electrode surface at bifunctional mechanism as described above. CO and Ru–OH molecules react at the anode surface. Previous studies and our results show that $Ru(OH)_{ad.}$ or $Ru(H_2O)_{ad.}$ particles on the leached-electrode create a catalytic effect for methanol oxidation. Fig. 4 shows that the methanol oxidation activity on C/NiZn and C/NiZn-Ru are significantly higher than on C/Ni electrode. Methanol oxidation peak current density values were obtained for C/Ni, C/NiZn and C/NiZn-Ru electrodes as 0.053, 0.300 and 0.459 A cm^{-2}, respectively. These values show ruthenium

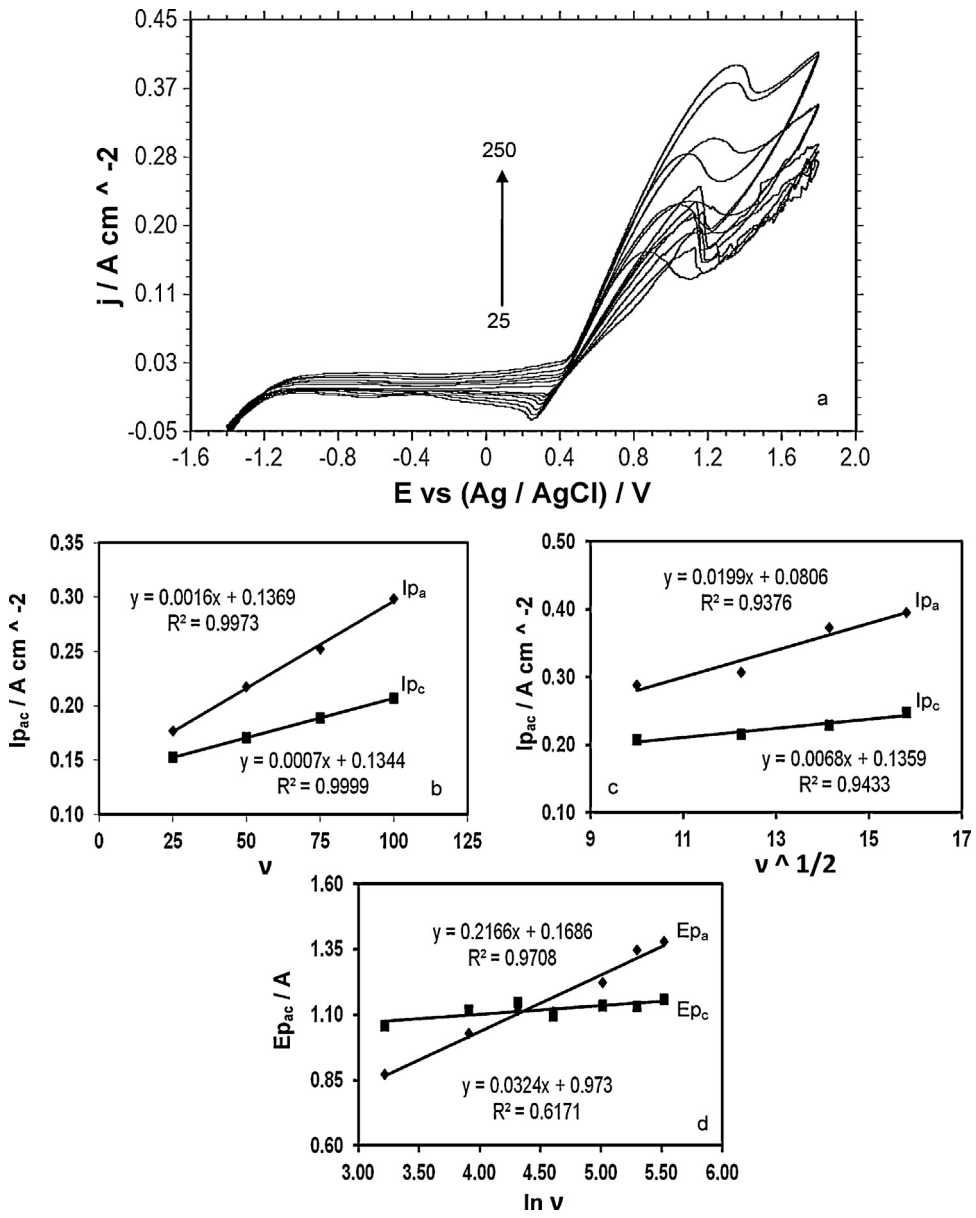

Fig. 5. **(a)** Cyclic voltammograms of methanol oxidation in 1.00 M CH_3OH + 1.00 M KOH at C/NiZn-Ru electrode at different scan rates: 25–250 mV s^{-1}. **(b)** Dependence of anodic (♦) and cathodic (■) peak currents to the sweep rate at lower values (25–100 mV s^{-1}). **(c)** The proportionality of anodic and cathodic peak currents to the square roots of sweep rate at higher values (100–250 mV s^{-1}). **(d)** Dependence of both anodic and cathodic E_p on ln υ.

deposited electrode has a higher methanol oxidation current than other electrodes. Additionally, the enhanced performance of C/NiZn and C/NiZn-Ru might be a result from the structural and chemical effects. High surface area with leached out zinc is responsible for the anodes as good electrocatalysts. The effects of large surface area and surface porosity were observed in our previous study as well [56].

Methanol oxidation occurs during anodic and the initial stage of the cathodic cycle [57]. Adsorbed methanol molecules are oxidized parallel to the oxidation of Ni^{2+} to Ni^{3+} species. The anodic current reaches maximum value at anodic scan. Methanol oxidation continues in reverse half cycle and methanol oxidation current goes maximum due to regeneration of active sites for methanol adsorption.

Fig. 5 represents the cyclic voltammetry curves of methanol oxidation (1.00 M) at different scan rates (υ = 25–250 mV s^{-1}) in 1.00 M KOH at C/NiZn-Ru electrode. Methanol oxidation peak current increases with increasing scan rate and potential shifts positive potential values. Methanol oxidation peak was observed at much more positive values than $Ni(OH)_2$ oxidation potential in higher scan rates.

The peak's currents are proportional to sweep rates in the range of 25–100 mV s^{-1} (Fig. 5b) pointing to the electrochemical activity of the surface redox couple. From the slope of these lines and using [58–60]

$$I_p = \left(\frac{n^2F^2}{4RT}\right)\nu A\Gamma^* \tag{16}$$

where $^*\Gamma$ is the surface coverage of the redox species (mol cm^{-2}) and ν being the potential sweep rate. The peak's currents were calculated by the nickel species for C/NiZn and C/NiZn-Ru electrodes as 1.93×10^{-8} mol cm^{-2} and 6.02×10^{-8} mol cm^{-2}, respectively. In the higher potential sweep rates (100–250 mV s^{-1}) this dependency is the square root form, Fig. 5c, defining domination of

diffusion controlled processes. Moreover, an electrochemical-chemical (EC) catalytic process occurs in Fig. 5c [61].

Fig. 5d shows the plot of E_p with respect to ln ν from the cyclic voltammograms recorded for C/NiZn electrode in 1.00 M methanol + 1.00 M KOH solution at potential sweep rates of 25–250 mV s^{-1} for anodic and cathodic peaks. As it is shown in Fig. 5d, the peak-to-peak separation ($\Delta E_p = E_{pa} - E_{pc}$, $\Delta E_p > 200/n$ mV, n is the number of the exchanged electrons) increases with the scan rate, indicating the limitation arising from charge transfer kinetics. According to Laviron theory, electron transfer coefficient (α) and charge transfer rate constant (k_s) for electron transfer process on the electrode surface were calculated from following equations [62]:

$$E_{pa} = E^o + \frac{RT}{(1-\alpha)nF} \ln\left[\frac{(1-\alpha)Fn\nu}{RTk_s}\right] \quad (17)$$

$$E_{pc} = E^o + \frac{RT}{\alpha nF} \ln\left[\frac{\alpha Fn\nu}{RTk_s}\right] \quad (18)$$

$$\ln\ k_s = \alpha \ln(1-\alpha) + (1-\alpha)\ln\alpha - \ln\frac{RT}{nF\nu} - \frac{\alpha(1-\alpha)nF\,\Delta E_p}{RT} \quad (19)$$

Fig. 5d shows E_p plot with respect to ln ν from the CVs recorded for C/NiZn-Ru catalyst in 1.00 M KOH in the presence of 1.00 M methanol at potential scan rates of 100–250 mV s^{-1} for anodic and cathodic peaks. Using the plot and Eqs. (17)–(19), anodic electron transfer coefficient (α_a) 0.12, cathodic electron transfer coefficient (α_c) 0.79 and ks were determined as 0.13 s^{-1}. It could mean the oxidation and reduction processes might not be the same from the α_a and α_c results [63,64]. Because the ΔE_p value was smaller than $200/n$ mV, α_a and α_c were not calculated for C/NiZn.

The temperature effect for methanol electrooxidation was determined from 298 to 318 K by means of CV. Fig. 6a shows CVs that methanol oxidation was carried out at various temperatures at C/NiZn-Ru. All CVs for methanol oxidation, oxidation peak currents increase with increasing temperature. Fig. 6b shows Arrhenius plots for methanol oxidation current on C/NiZn and C/NiZn-Ru electrode. Activation energy (E_a) values were calculated for C/NiZn and C/NiZn-Ru electrode according to the Arrhenius equation. E_a values of C/NiZn and C/NiZn-Ru electrode is 23.96 and 5.94 kJ/mol, respectively.

Fig. 7 presents methanol concentrations effect on the CVs of C/NiZn-Ru electrode in 1.00 M KOH solution. In Fig. 7, CV curves in 1.00 M KOH at a 100 mV s^{-1} scan rate for methanol concentrations ranging from 0.10 to 1.00 M were received. Methanol oxidation peak current increases with increasing methanol concentration.

3.3. Electrochemical impedance spectroscopy (EIS) measurements

In order to further investigate the methanol oxidation mechanism, electrochemical impedance spectroscopy (EIS) was performed on the C/Ni (Fig. 8a), C/NiZn (Fig. 8b) and C/NiZn-Ru (Fig. 8c) electrodes at the 0.60 V potential. Nyquist plots for methanol oxidation in 1.00 M CH_3OH + 1.00 M KOH solution at 298 K are shown in Fig. 8. The EIS responses change with the C/Ni, C/NiZn and C/NiZn-Ru catalysts at 0.60 V potential. In Fig. 8a, one large depressed capacitive loop at the high-frequency region and an inductive loop at the low-frequency region were observed. The capacitive loop in the high-frequency region is related to the charge transfer resistance and diffuse layer resistance and the low frequency inductive behavior can be explained by change in polarity of alcohol products moved away from the surface [65]. In Fig. 8b and c, there are a loop and linear portion of this curve. Linear portion related to methanol oxidation reaction is diffusion controlled [66]. In addition, the linear part of surrounding the surface is due to collection in the diffusion layer [15,66–74].

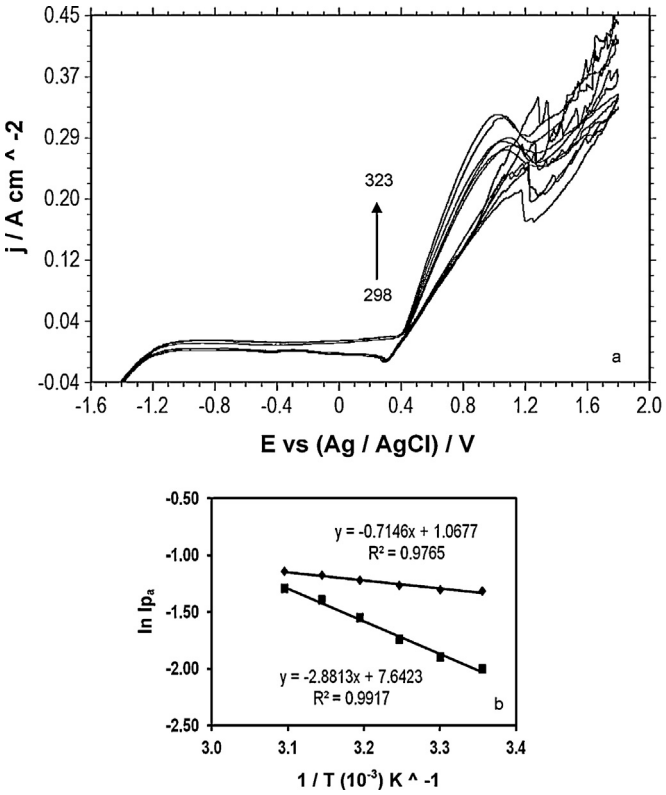

Fig. 6. **(a)** Cyclic voltammograms for the methanol oxidation reaction on C/NiZn-Ru electrode at scan rates of 100 mV s^{-1} in 1.00 M CH_3OH + 1.00 M KOH at 298, 303, 308, 313 and 318 K temperatures. **(b)** $1/T - \ln I_p$ curves obtained in 1.00 M KOH solution containing 1.00 M methanol on C/NiZn (■) and C/NiZn-Ru (♦) electrodes at 100 mV s^{-1} scan rate.

Scheme 1 presents EIS data which were fitted by electrical equivalent circuit diagrams. In Scheme 1, R_{ct}, which corresponds to charge transfer resistance and R_s, CPE, and n represent solution resistance, a constant phase element and the phase shift, respectively. The CPE was used in place of a double-layer capacitance (C_{dl}) in order to obtain a more accurate fit of the experimental results [75–79]. In addition, R_{ads}, L and C_{ads} signify surface adsorption resistance, inductance and a capacitance representing the adsorption process. Total polarization resistance was indicated as $R_p = R_{ct} + R_{ads}(R^*_{ads})$. C/Ni electrode's polarization resistance and

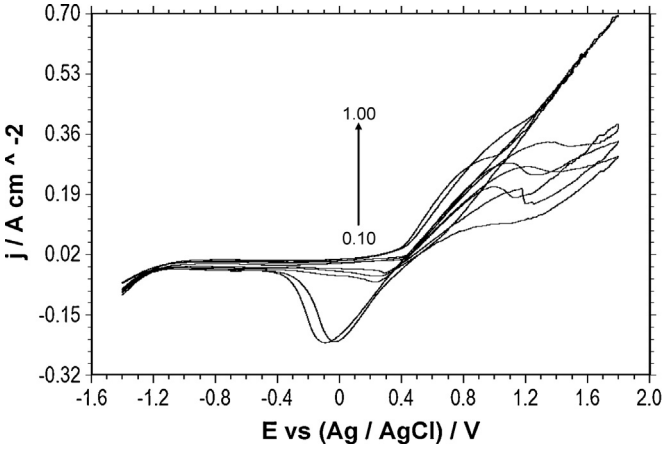

Fig. 7. Cyclic voltammograms for the methanol oxidation reaction on C/NiZn-Ru electrode at scan rates of 100 mV s^{-1} in 1.00 M KOH solutions that contain concentrations of CH_3OH 0.00 M, 0.10 M, 0.25 M, 0.50 M, 0.75 M and, 1.00 M.

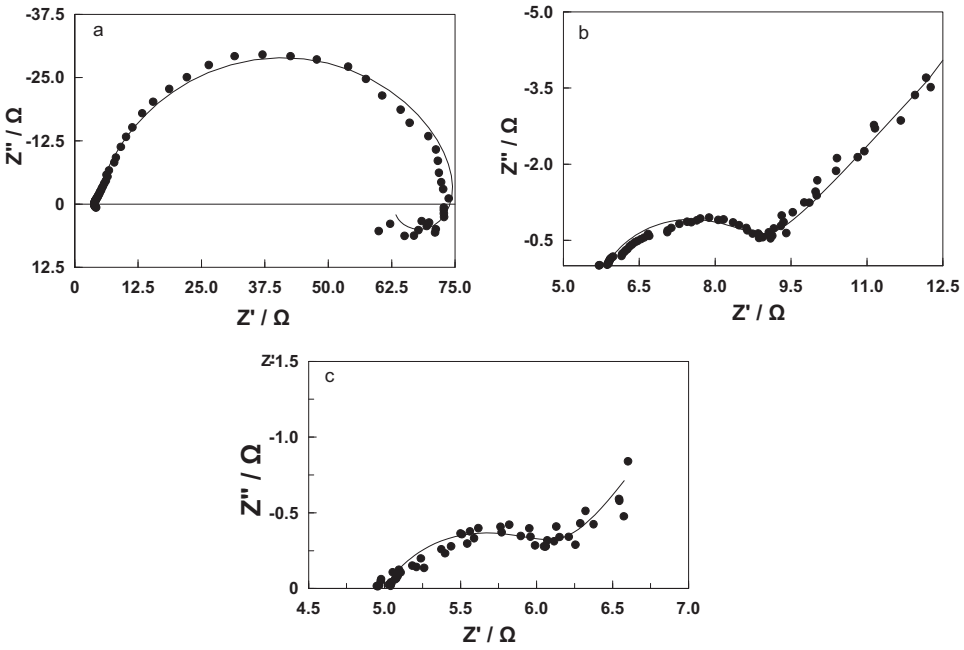

Fig. 8. Nyquist plots for the methanol oxidation reaction at 0.60 V on C/Ni (a), C/NiZn (b) and C/NiZn-Ru (c) electrodes at 298 K in 1.00 M CH_3OH + 1.00 M KOH (solid line shows the fitted results).

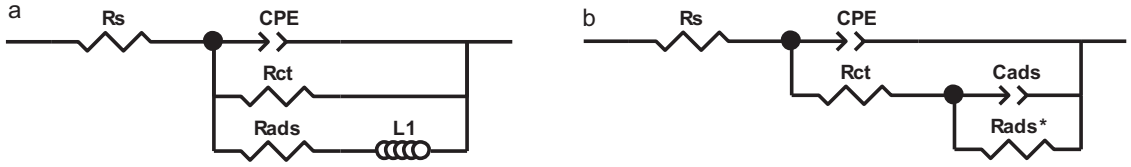

Scheme 1. Equivalent circuit compatible with the Nyquist diagrams in Fig. 8.

diameter of a capacitive loop were about 92.3 Ω. Fig. 8b indicates the Nyquist plots of C/NiZn. Fig. 8b and c show, a small depressed capacitive semicircle with an approximate diameter of 6.75 and 1.67 Ω, respectively. These are demonstrated that there is a fast electron-transfer rate on the C/NiZn and C/NiZn-Ru.

The higher activity of the C/NiZn-Ru can be related to the synergistic effect of Ni and Zn, surface porosity, enhancement of the surface area after the leaching process and addition of ruthenium deposits [80–83]. The zinc is not completely leached out on electrode surface, but small amount of zincs on surface changes the "d" band structure to increase the exchange current density without displaying electrochemical properties of zinc [84].

3.4. Chronoamperometric measurements

In Fig. 9, chronoamperograms were recorded on C/Ni, C/NiZn and C/NiZn-Ru electrodes for 1 h at 0.60 V potential in 1.00 M CH_3OH + 1.00 M KOH are given. As time progresses, methanol oxidation current initially decreases and remains constant. At first, the active sites are free of adsorbed methanol molecules (fast kinetic rate reaction); after that, the adsorption of new methanol molecules is a function of the liberation of the active sites by methanol oxidation or intermediate species, such as CO, CH_x and CH_3O formed during the first minutes (rate determining step) [85] that are responsible for poisoning of the catalytic sites. The results imply that the C/NiZn-Ru electrode exhibits higher stability than C/NiZn electrode.

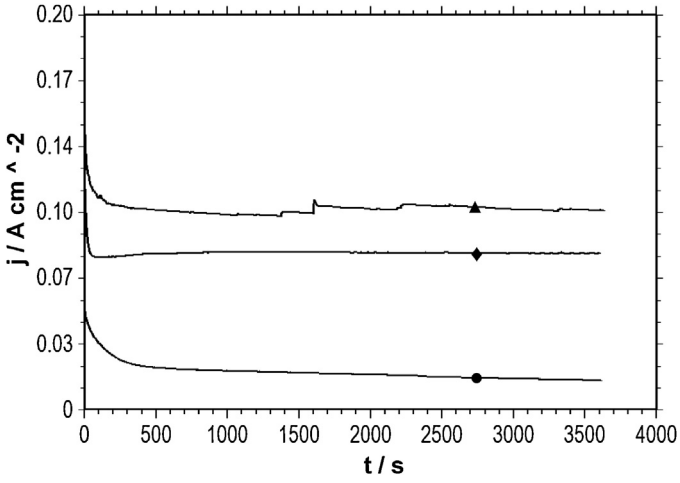

Fig. 9. Chronoamperograms for methanol oxidation reaction potential at 298 K and 0.60 V in 1.00 M CH_3OH + 1.00 M KOH. Curves correspond to (●) C/Ni, (♦) C/NiZn, (▲) C/NiZn-Ru.

4. Conclusions

The methanol oxidation on C/NiZn and C/NiZn-Ru electrodes was investigated in 1.00 M KOH solution. Both C/NiZn and C/NiZn-Ru electrodes showed electrocatalytic effects for methanol

oxidation reaction while the C electrode displayed no activity. The results exhibited that the methanol oxidation on the C/NiZn-Ru electrode was faster than on the C/NiZn electrode. Additionally, the C/NiZn and C/NiZn-Ru electrodes' methanol oxidation peak current densities were determined as 0.300 and 0.459 A cm^{-2}, respectively. The C/NiZn-Ru electrode combined with the lower-charge transfer resistance presents the most conductive surface for methanol oxidation in KOH, according to Nyquist's plots. Chronoamperogram results of electrodes proved that the C/NiZn-Ru electrode shows both high-current density and stability with time in same potential. It was shown that a C/NiZn-Ru electrode has stability, low costs, high-current density and electrocatalytic activity for methanol oxidation reactions.

Acknowledgement

The authors are greatly thankful to Cukurova University research fund (Project Number: FEF2009D9) for financial support.

References

[1] Z. Tang, Q. Li, G. Lu, The effect of plasma pre-treatment of carbon used as a Pt catalyst support for methanol electrooxidation, Carbon 45 (2007) 41.
[2] Y. Lu, R.G. Reddy, Electrocatalytic properties of carbon supported cobalt phthalocyanine-platinum for methanol electro-oxidation, International Journal of Hydrogen Energy 33 (2008) 3930.
[3] M. Jafarian, R.B. Moghaddam, M.G. Mahjani, F. Gobal, Electro-catalytic oxidation of methanol on a Ni-Cu alloy in alkaline medium, Journal of Applied Electrochemistry 36 (2006) 913.
[4] C. Qiu, R. Shang, Y. Xie, Y. Bu, C. Li, H. Ma, Electrocatalytic activity of bimetallic Pd-Ni thin films towards the oxidation of methanol and ethanol, Materials Chemistry and Physics 120 (2010) 323.
[5] M. Wang, W. Liu, C. Huang, Investigation of PdNiO/C catalyst for methanol electrooxidation, International Journal of Hydrogen Energy 34 (2009) 2758.
[6] R.M.A. Hameed, K.M. El-Khatib, Ni-P and Ni-Cu-P modified carbon catalysts for methanol electro-oxidation in KOH solution, International Journal of Hydrogen Energy 35 (2010) 2517.
[7] A.L. Dicks, The role of carbon in fuel cells, Journal of Power Sources 156 (2006) 128.
[8] I. Danaee, M. Jafarian, A. Mirzapoor, F. Gobal, M.G. Mahjani, Electrooxidation of methanol on NiMn alloy modified graphite electrode, Electrochimica Acta 55 (2010) 2093.
[9] D. Geng, D. Matsuki, J. Wang, T. Kawaguchi, W. Sugimoto, Y. Takasu, Activity and durability of ternary PtRuIr/C for methanol electro-oxidation, Journal of the Electrochemical Society 156 (2009) B397.
[10] X. Zhang, H. Wang, J. Key, V. Linkov, S. Ji, X. Wang, Z. Lei, R. Wang, Strain effect of core-shell Co@Pt/C nanoparticle catalyst with enhanced electrocatalytic activity for methanol oxidation, Journal of the Electrochemical Society 159 (2012) B270.
[11] I. Danaee, M. Jafarian, F. Forouzandeh, F. Gobal, M.G. Mahjani, Electrocatalytic oxidation of methanol on Ni and NiCu alloy modified glassy carbon electrode, International Journal of Hydrogen Energy 33 (2008) 4367.
[12] H.B. Hassan, Z.A. Hamid, Electroless Ni-B supported on carbon for direct alcohol fuel cell applications, International Journal of Hydrogen Energy 36 (2011) 849.
[13] Y. Zhao, X. Yang, J. Tian, F. Wang, L. Zhan, Methanol electro-oxidation on Ni@Pd core-shell nanoparticles supported on multi-walled carbon nanotubes in alkaline media, International Journal of Hydrogen Energy 35 (2010) 3249.
[14] A.A. Aal, H.B. Hassan, M.A.A. Rahim, Nanostructured Ni-P-TiO_2 composite coatings for electrocatalytic oxidation of small organic molecules, Journal of Electroanalytical Chemistry 619–620 (2008) 17.
[15] I. Danaee, M. Jafarian, F. Forouzandeh, F. Gobal, M.G. Mahjani, Electrochemical impedance studies of methanol oxidation on GC/Ni and GC/NiCu electrode, International Journal of Hydrogen Energy 34 (2009) 859.
[16] M.V. Ananth, N.V. Parthasaradhy, Hydrogen evolution characteristics of electrodeposited Ni-Zn-Fe coatings in alkaline solutions, International Journal of Hydrogen Energy 22 (1997) 747.
[17] R. Solmaz, G. Kardaş, Electrochemical deposition, characterization and application of NiCoZn coatings as effective cathode materials for hydrogen production, in: 215th ESC Meeting, San Francisco, CA, 2009.
[18] R. Solmaz, A. Döner, G. Kardaş, Electrochemical deposition and characterization of NiCu coatings as cathode materials for hydrogen evolution reaction, Electrochemistry Communications 10–12 (2008) 1909.
[19] R. Solmaz, A. Döner, G. Kardaş, The stability of hydrogen evolution activity and corrosion behavior of NiCu coatings with long-term electrolysis in alkaline solution, International Journal of Hydrogen Energy 34 (2009) 2089.
[20] C.C. Hu, C.H. Tsay, A. Bai, Optimization of the hydrogen evolution activity on zinc-nickel deposits using experimental strategies, Electrochimica Acta 48 (2003) 907.
[21] R. Solmaz, A. Döner, İ. Şahin, A.O. Yüce, G. Kardaş, B. Yazıcı, The stability of NiCoZn electrocatalyst for hydrogen evolution activity in alkaline solution during long-term electrolysis, International Journal of Hydrogen Energy 34 (2009) 7910.
[22] A. Seghiouer, J. Chevalet, A. Barhoun, F. Lantelme, Electrochemical oxidation of nickel in alkaline solutions: a voltammetric study and modelling, Journal of Electroanalytical Chemistry 442 (1998) 113.
[23] J.L. Weininger, M.W. Breiter, Effect of crystal structure on the anodic oxidation of nickel, Journal of The Electrochemical Society 110 (1963) 484.
[24] M. Vukovic, Voltammetry and anodic stability of a hydrous oxide film on a nickel electrode in alkaline solution, Journal of Applied Electrochemistry 24 (1994) 878.
[25] O. Enea, Molecular structure effects in electrocatalysis—II. Oxidation of d-glucose and of linear polyols on Ni electrodes, Electrochimica Acta 35 (1990) 375.
[26] M. Fleischmann, K. Korinek, D. Pletcher, The oxidation of organic compounds at a nickel anode in alkaline solution, Journal of Electroanalytical Chemistry 31 (1971) 39.
[27] J.B. Raoof, M.A. Karimi, S.R. Hosseini, S. Mangelizadeh, Cetyltrimethyl ammonium bromide effect on highly electrocatalysis of methanol oxidation based on nickel particles electrodeposited into poly (m-toluidine) film on the carbon paste electrode, Journal of Electroanalytical Chemistry 638 (2010) 33.
[28] M.A.A. Rahim, R.M.A. Hameed, M.W. Khalil, Nickel as a catalyst for the electro-oxidation of methanol in alkaline medium, Journal of Power Sources 134 (2004) 160.
[29] M.A.A. Rahim, R.M.A. Hameed, M.W. Khalil, The role of a bimetallic catalyst in enhancing the electro-catalytic activity towards methanol oxidation, Journal of Power Sources 135 (2004) 42.
[30] M. Jafarian, M. Babaee, F. Gobal, M.G. Mahjani, Electro-oxidation of alcohols on nickel dispersed in poly-o-aminophenol modified graphite electrode, Journal of Electroanalytical Chemistry 652 (2011) 8.
[31] Q. Yi, W. Huang, J. Zhang, X. Liu, L. Li, Methanol oxidation on titanium-supported nano-scale Ni flakes, Catalysis Communications 9 (2008) 2053.
[32] A.V. Tripkovic', K.D. Popovic', B.N. Grgur, B. Blizanac, P.N. Ross, N.M. Markovic, Methanol electrooxidation on supported Pt and PtRu catalysts in acid and alkaline solutions, Electrochimica Acta 47 (2002) 3707.
[33] S.H. Bonilla, C.F. Zinola, J. Rodríguez, V. Díaz, M. Ohanian, S. Martínez, B.F. Giannetti, Catalytic effects of ruthenium and osmium spontaneous deposition on platinum surfaces toward methanol oxidation, Journal of Colloid and Interface Science 288 (2005) 377.
[34] D. He, L. Yang, S. Kuang, Q. Cai, Fabrication and catalytic properties of Pt and Ru decorated TiO_2\CNTs catalyst for methanol electrooxidation, Electrochemistry Communications 9 (2007) 2467.
[35] M.C. Santos, A.J. Terezo, V.C. Fernandes, E.C. Pereira, L.O.S. Bulhões, An EQCM investigation of charging RuO_2 thin films prepared by the polymeric precursor method, Journal of Solid State Electrochemistry 9 (2005) 91.
[36] M.C. Santos, L. Cogo, S.T. Tanimoto, M.L. Calegaro, L.O.S. Bulhões, A nanogravimetric investigation of the charging processes on ruthenium oxide thin films and their effect on methanol oxidation, Applied Surface Science 253 (2006) 1817.
[37] W. Sugimoto, T. Saida, Y. Takasu, Co-catalytic effect of nanostructured ruthenium oxide towards electro-oxidation of methanol and carbon monoxide, Electrochemistry Communications 8 (2006) 411.
[38] H. Huang, W. Li, H. Liu, Effect of treatment temperature on structures and properties of zirconia-supported ruthenium oxide catalysts for selective oxidation of methanol to methyl formate, Catalysis Today 183 (2012) 58.
[39] E.V. Spinacé, A.O. Neto, M. Linardi, Electro-oxidation of methanol and ethanol using PtRu/C electrocatalysts prepared by spontaneous deposition of platinum on carbon-supported ruthenium nanoparticles, Journal of Power Sources 129 (2004) 121.
[40] C.-H. Lee, S.-E. Bae, C.-W. Lee, D.-H. Jung, C.-S. Kim, D.-R. Shin, Electrooxidation of methanol on ruthenium oxide layer supported by basal plane graphite in acid media, International Journal of Hydrogen Energy 26 (2001) 175.
[41] Y. Ishikawa, M.-S. Liao, C.R. Cabrera, Oxidation of methanol on platinum, ruthenium and mixed Pt–M metals (M = Ru, Sn): a theoretical study, Surface Science 463 (2000) 66.
[42] L.-M. Huang, T.-C. Wen, Platinum–ruthenium nanoparticles in poly(2,5-dimethoxyaniline)-poly (styrene sulfonic acid) via one-step synthesis route for methanol oxidation, Journal of Power Sources 182 (2008) 32.
[43] S.-Y. Huang, C.-M. Chang, C.-T. Yeh, Promotion of platinum–ruthenium catalyst for electro-oxidation of methanol by ceria, Journal of Catalysis 241 (2006) 400.
[44] K. Lasch, L. Jörissen, J. Garche, The effect of metal oxides as co-catalysts for the electro-oxidation of methanol on platinum–ruthenium, Journal of Power Sources 84 (1999) 225.
[45] M. Watanabe, S. Motoo, Electrocatalysis by ad-atoms. Part II Enhancement of the oxidation of carbon monoxide on platinum by ruthenium ad-atoms, Journal of Electroanalytical Chemistry 60 (1975) 267.
[46] F. Vigier, F. Gloaguen, J.-M. Le'ger, C. Lamy, Electrochemical and spontaneous deposition of ruthenium at platinum electrodes for methanol oxidation: an electrochemical quartz crystal microbalance study, Electrochimica Acta 46 (2001) 4331.
[47] S.H. Bonilla, C.F. Zinola, J. Rodríguez, V. Díaz, M. Ohanian, S. Martínez, B.F. Giannetti, Catalytic effects of ruthenium and osmium spontaneous deposition on platinum surfaces toward methanol oxidation, Journal of Colloid and Interface Science 288 (2005) 377.
[48] S.C. Chang, L.W.H. Leung, M.J. Weaver, Metal crystallinity effects in electrocatalysis as probed by real-time FTIR spectroscopy: electrooxidation of formic acid,

methanol and ethanol on ordered low-index platinum surfaces, The Journal of Physical Chemistry 94 (1990) 6013.
[49] J. Jiang, A. Kucernak, Electrooxidation of small organic molecules on mesoporous precious metal catalysts II: CO and methanol on platinum-ruthenium alloy, Journal of Electroanalytical Chemistry 543 (2003) 187.
[50] G. Tremiliosi-Filho, H. Kim, W. Chrzanowski, A. Wieckowski, B. Grzybowska, P. Kulesza, Reactivity and activation parameters in methanol oxidation on platinum single crystal electrodes decorated by ruthenium adlayers, Journal of Electroanalytical Chemistry 467 (1999) 143.
[51] H.N. Dinh, X. Ren, F.H. Garzon, P. Zelenay, S. Gottesfeld, Electrocatalysis in direct methanol fuel cell: in-situ probing of PtRu anode catalyst surfaces, Journal of Electroanalytical Chemistry 491 (2000) 222.
[52] M. Krausa, W. Vielstich, Study of the electrocatalytic influence of Pt:Ru and Ru on the oxidation of residues of small organic molecules, Journal of Electroanalytical Chemistry 379 (1994) 307.
[53] T. Frelink, W. Visscher, J.A.R. Vanveen, On the role of Ru and Sn as promoters of methanol electro-oxidation over Pt, Surface Science 335 (1995) 353.
[54] T. Frelink, W. Visscher, J.A.R. Vanveen, Measurement of the Ru surface content of electrodeposited PtRu electrodes with the electrochemical quartz crystal microbalance: implications for methanol and CO electrooxidation, Langmuir 12 (1996) 3702.
[55] P. Waszczuk, G.Q. Lu, A. Wieckowski, C. Lub, C. Rice, R.I. Masel, UHV and electrochemical studies of CO and methanol adsorbed at platinum/ruthenium surfaces, and reference to fuel cell catalysis, Electrochimica Acta 47 (2002) 3637.
[56] E. Telli, R. Solmaz, G. Kardaş, Electrocatalytic oxidation of methanol on Pt/NiZn electrode in alkaline medium, Russian Journal of Electrochemistry 47 (2011) 811.
[57] A. Döner, E. Telli, G. Kardaş, Electrocatalysis of Ni-promoted Cd coated graphite toward methanol oxidation in alkaline medium, Journal of Power Sources 205 (2012) 71.
[58] A.J. Bard, L.R. Faulkner, Electrochemical Methods, Fundamentals and Applications, Wiley, New York, 2001, pp. 591.
[59] J.B. Raoof, R. Ojani, S.R. Hosseini, A novel, effective and low cost catalyst for methanol oxidation based on nickel ions dispersed onto poly(o-toluidine)/Triton X-100 film at the surface of multi-walled carbon nanotube paste electrode, Journal of Power Sources 196 (2011) 1855.
[60] N. Sattarahmady, H. Heli, F. Faramarzi, Nickel oxide nanotubes-carbon microparticles/Nafion nanocomposite for the electrooxidation and sensitive detection of metformin, Talanta 82 (2010) 1126.
[61] R.S. Nicholson, I. Shain, Theory of stationary electrode polarography single scan and cyclic methods applied to reversible, irreversible, and kinetic systems, Analytical Chemistry 36 (1964) 706.
[62] E. Laviron, General expression of the linear potential sweep voltammogram in the case of diffusionless electrochemical systems, Journal of Electroanalytical Chemistry 101 (1979) 19.
[63] H. Luo, Z. Shi, N. Li, Z. Gu, Q. Zhuang, Investigation of the electrochemical and electrocatalytic behavior of single-wall carbon nanotube film on a glassy carbon electrode, Analytical Chemistry 73 (2001) 915.
[64] M. Hajjizadeh, A. Jabbari, H. Heli, A.A. Moosavi, A. Shafiee, K. Karimian, Electrocatalytic oxidation and determination of deferasirox and deferiprone on a nickel oxyhydroxide-modified electrode, Analytical Biochemistry 373 (2008) 337.
[65] G. Kardaş, B. Yazıcı, M. Erbil, Effect of some primary alcohols on hydrogen yield on platinum cathode in chloride solution, International Journal of Hydrogen Energy 28 (2003) 1213.
[66] M. Erbil, The determination of corrosion rates by analysis of A.C. impedance diagrams, Chimica Acta Turcica 1 (1988) 60.
[67] M.G. Mahjani, A. Ehsani, M. Jafarian, Electrochemical study on the semiconductor properties and fractal dimension of poly ortho aminophenol modified graphite electrode in contact with different aqueous electrolytes, Synthetic Metals 160 (2010) 1252.
[68] K.L. Nagashree, N.H. Raviraj, M.F. Ahmed, Carbon paste electrodes modified by Pt and Pt-Ni microparticles dispersed in polyindole film for electrocatalytic oxidation of methanol, Electrochimica Acta 55 (2010) 2629.
[69] M. Chen, C.Y. Du, G.P. Yin, P.F. Shi, T.S. Zhao, Numerical analysis of the electrochemical impedance spectra of the cathode of direct methanol fuel cell, International Journal of Hydrogen Energy 34 (2009) 1522.
[70] W. Sugimoto, K. Aoyama, T. Kawaguchi, Y. Murakami, Y. Takasu, Kinetics of CH_3OH oxidation on PtRu/C studied by impedance and CO stripping voltammetry, Journal of Electroanalytical Chemistry 576 (2005) 215.
[71] Z.-B. Wang, Y.-Y. Chu, A.-F. Shao, P.-J. Zuo, G.-P. Yin, Electrochemical impedance studies of electrooxidation of methanol and formic acid on Pt/C catalyst in acid medium, Journal of Power Sources 190 (2009) 336.
[72] C.-M. Lai, J.-C. Lin, K.-L. Hsueh, C.-P. Hwang, K.-C. Tsay, L.-D. Tsai, Y.-M. Peng, On the electrochemical impedance spectroscopy of direct methanol fuel cell, International Journal of Hydrogen Energy 32 (2007) 4381.
[73] J.T. Müller, P.M. Urban, W.F. Hölderich, Impedance studies on direct methanol fuel cell anodes, Journal of Power Sources 84 (1999) 157.
[74] S.-H. Yang, C.-Y. Chen, W.-J. Wang, An impedance study of an operating direct methanol fuel cell, Journal of Power Sources 195 (2010) 2319.
[75] I. Danaee, M. Jafarian, F. Forouzandeh, F. Gobal, M.G. Mahjani, Kinetic interpretation of a negative time constant impedance of glucose electrooxidation, The Journal of Physical Chemistry B 112 (2008) 15933.
[76] D. Chakraborty, I.B. Chorkendorff, T. Johannessen, Metamorphosis of the mixed phase PtRu anode catalyst for direct methanol fuel cells after exposure of methanol: In situ and ex situ characterizations, Journal of Power Sources 173 (2007) 110.
[77] R.D. Armstrong, M. Henderson, The impedance of transpassive chromium, Journal of Electroanalytical Chemistry 40 (1972) 121.
[78] F. Seland, R. Tunold, D.A. Harrington, Impedance study of methanol oxidation on platinum electrodes, Electrochimica Acta 51 (2006) 3827.
[79] E. Barsoukov, J.R. Macdonald, Impedance spectroscopy: Theory, Experiment and Application, Wiley, New Jersey, 2005.
[80] S.M. Miulovic, S.Lj. Maslovara, I.M. Perovic, V.M. Nikolic, M.P. Marceta Kaninski, Electrocatalytic activity of ZnCoMo based ionic activators for alkaline hydrogen evolution—Part II, Applied Catalysis A: General 451 (2013) 220.
[81] C. Hitz, A. Lasia, Experimental study and modeling of impedance of the her on porous Ni electrodes, Journal of Electroanalytical Chemistry 500 (2001) 213.
[82] R. Solmaz, A. Döner, G. Kardaş, Preparation, characterization and application of alkaline leached CuNiZn ternary coatings for long-term electrolysis in alkaline solution, International Journal of Hydrogen Energy 35 (2010) 10045.
[83] I. Herraiz-Cardona, E. Ortega, V. Pérez-Herranz, Impedance study of hydrogen evolution on Ni/Zn and Ni–Co/Zn stainless steel based electrodeposits, Electrochimica Acta 56 (2011) 1308.
[84] M.V. Ananth, N.V. Parthasaradhy, Hydrogen evolution characterristics of electrodeposited Ni-Zn-Fe coatings in alkaline solutions, International Journal of Hydrogen Energy 22 (1997) 747.
[85] E. Antolini, Platinum-based ternary catalysts for low temperature fuel cells Part II. Electrochemical properties, Applied Catalysis B: Environmental 74 (2007) 337.